

# Novel Bis-C,N-Cyclometalated Iridium(III) Thiosemicarbazide Antitumor Complexes: Interactions with Human Serum Albumin and DNA, and Inhibition of Cathepsin B

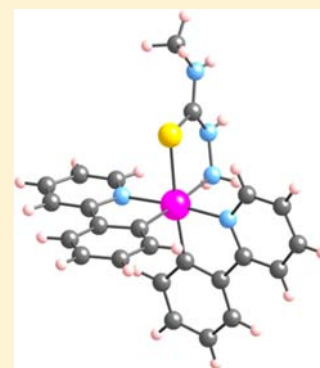
José Ruiz,<sup>\*,†</sup> Consuelo Vicente,<sup>†</sup> Concepción de Haro,<sup>†</sup> and Delia Bautista<sup>‡</sup>

<sup>†</sup>Departamento de Química Inorgánica and Regional Campus of International Excellence "Campus Mare Nostrum", Universidad de Murcia and Instituto Murciano de Investigación Biosanitaria (IMIB), E-30071- Murcia, Spain

<sup>‡</sup>SAI, Universidad de Murcia, E-30100-Murcia, Spain

## S Supporting Information

**ABSTRACT:** A series of new organoiridium(III) complexes  $[\text{Ir}(\text{N}-\text{C})_2(\text{N}-\text{S})]\text{Cl}$  (HN-C = 2-phenylpyridine (Hppy), N-S = methyl thiosemicarbazide (1), phenyl thiosemicarbazide (2) and naphthyl thiosemicarbazide (3)) have been synthesized and characterized. The crystal structure of (1) has been established by X-ray diffraction, showing the thiosemicarbazide ligand bound to the iridium atom as N,S-chelate. The cytotoxicity studies show that they are more active than cisplatin (about 5-fold) in T47D (breast cancer) at 48 h incubation time. On the other hand, very low resistance factors (RF) of 1–3 in A2780cisR (cisplatin-resistant ovarian carcinoma) at 48 h were observed ( $\text{RF} \approx 1$ ). Ir accumulation in T47D cell line after 48 h continuous exposure for complexes 1–3 are higher than that corresponding to cisplatin (about 10 times). The complexes 1–3 bind strongly to HSA with binding constants of about  $10^4 \text{ M}^{-1}$  at 296 K, binding occurring at the warfarin site I for 2. Complexes 2 and 3 are also capable of binding in the minor groove of DNA as shown by Hoechst 33258 displacement experiments. Furthermore, complex 2 is also a good cathepsin B inhibitor (an enzyme implicated in a number of cancer related events), being the enzyme reactivated by cysteine.



## INTRODUCTION

Cisplatin is one of the antitumoral agents most used in clinical therapy.<sup>1–6</sup> However, it has a high general toxicity, and some tumors develop resistance to the drug. This limits the use of cisplatin to the treatment of ovarian, head and neck, bladder, and testicular tumors. For these reasons, the potential of other transition metal-based drugs as anticancer agents is being actively explored.<sup>7–13</sup>

Organometallic complexes offer enormous scope for the design of anticancer drug candidates, in spite of such compounds having long been considered to be unstable under physiological conditions. Thus, investigations of the cytotoxic properties of arene ruthenium(II) complexes such as  $[\text{Ru}(\eta^6\text{-arene})\text{Cl}_2(\text{PTA})]$  (RAPTA; PTA = 1,3,5-triaza-7-phosphatricyclo-[3.3.1.1]decane) and  $[\text{Ru}(\eta^6\text{-arene})(\text{en})\text{Cl}]^+$  (en = ethylenediamine) have established promising anticancer activity.<sup>12–16</sup> On the other hand, Sadler et al. have recently found that replacement of the neutral N,N-bound chelating ligand bpy by the negatively charged C,N-bound 2-phenylpyridine (ppy) ligand in an iridium(III) chlorido complex can also switch on biological activity.<sup>17,18</sup> In general iridium(III) complexes are usually thought to be relatively inert and can be used as biomolecular and cellular probes.<sup>19</sup> Thus for example, to design new biological probes for bovine serum albumin (BSA), Lo et al. prepared a series of luminescent cyclometalated Ir(III) complexes containing an indole derivative (indole is known to bind to BSA) which were found to be

highly cytotoxic toward HeLa cells.<sup>20</sup> Furthermore, the synthesis of some cyclometalated pyridynaphthalimide iridium(III) complexes as protein kinase inhibitors has been also recently reported.<sup>21</sup> A number of C,N-cyclometalated antitumor compounds of Ru, Rh, Ir, and Pt have been prepared recently by our group.<sup>22–26</sup>

We report herein the synthesis and cytotoxic activity of a series of new nonconventional organoiridium(III) complexes of the type  $[\text{Ir}(\text{N}-\text{C})_2(\text{N}-\text{S})]\text{Cl}$  (HN-C = 2-phenylpyridine (Hppy), N-S = thiosemicarbazide). Values of  $\text{IC}_{50}$  were studied for the new organoiridium(III) complexes against a panel of human tumor cell lines representative of ovarian (A2780 and A2780cisR), and breast cancer (T47D, cisplatin resistant). The interaction of the new Ir(III) thiosemicarbazide complexes toward human serum albumin (HSA, which is a transport carrier for drugs) and DNA, and also their behavior as cathepsin B inhibitors (a type of enzymes that are overexpressed in many cancer cell lines) have also been studied.

## RESULTS AND DISCUSSION

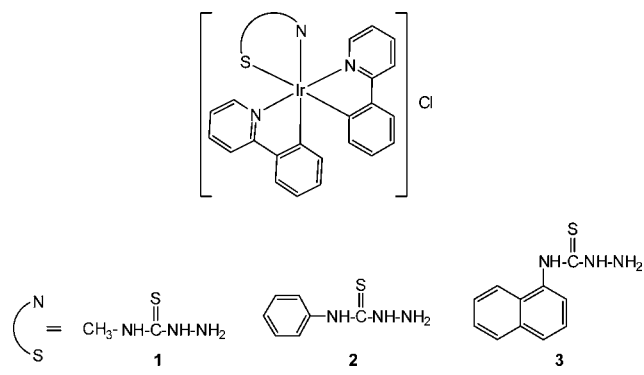
**Synthesis of the New Iridium Compounds  $[\text{Ir}(\text{N}-\text{C})_2(\text{N}-\text{S})]\text{Cl}$ .** The organoiridium(III) complexes were prepared from the reaction of  $[\text{Ir}_2(\text{N}-\text{C})_4\text{Cl}_2]$  (HN-C = Hppy) with the corresponding thiosemicarbazide in 1:2 molar ratio in a

Received: October 11, 2012

Published: January 9, 2013

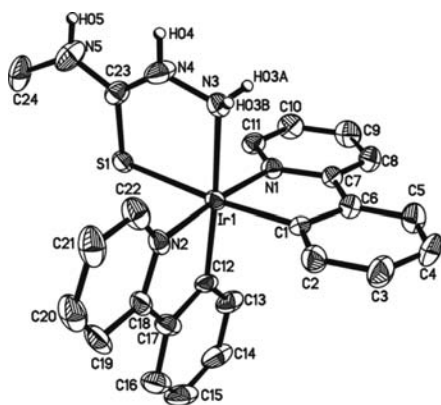
mixture of EtOH and CH<sub>2</sub>Cl<sub>2</sub> (Chart 1). All the complexes were characterized by <sup>1</sup>H NMR spectroscopy, positive-ion ESI-

Chart 1



MS, and IR spectroscopy and gave satisfactory elemental analyses. The assignments were confirmed by COSY, NOESY, DEPT, and HSQC. No attempts to isolate enantiomerically pure complexes 1–3 have been undertaken (Ir(III) center being stereogenic).

**X-ray Crystal Structure of Complex 1.** The crystal structure of 1 has been established by X-ray diffraction (Figure 1). The iridium(III) center adopts a distorted octahedral



**Figure 1.** ORTEP plot (ellipsoids drawn at 50% probability level) of complex 1. Selected bond lengths (Å) and angles (deg): Ir1–C1 = 2.025(3), Ir1–C12 = 2.013(3), Ir1–N1 = 2.055(3), Ir1–N2 = 2.043(3), Ir1–N3 = 2.180(3), Ir1–S1 = 2.4132(8), C1–Ir1–N1 = 80.05(12), C12–Ir1–N2 = 80.71(13), S1–Ir1–N3 = 81.75(18).

geometry. The thiosemicarbazide ligand binds the iridium atom as N,S-chelate. The coordinating nitrogen atoms of the two ppy rings are in a trans arrangement, as found typically in the crystal structure of cyclometalated iridium complexes.<sup>27,28</sup> The values of the Ir–C and Ir–N bond distances of the bonded ppy ligands are within the normal ranges expected for such cyclometalated complexes.<sup>29,30</sup> C–Ir–N bite angles are about 80°. The trans-influence of the carbon donors renders a longer Ir–N bond length in the thiosemicarbazide ligand (Ir–N3 = 2.180(3) Å) than in the cyclometalating ligand. Supramolecular interactions such as S···H–C (Figure 2), Cl···H–C and Cl···H–N contacts are present in 1 (Supporting Information, Figure S1).

**Biological Activity: Cytotoxicity Studies.** The cytotoxicity of the iridium(III) complexes 1–3 was evaluated (Table 1) toward the T47D human breast cancer cell line (cisplatin

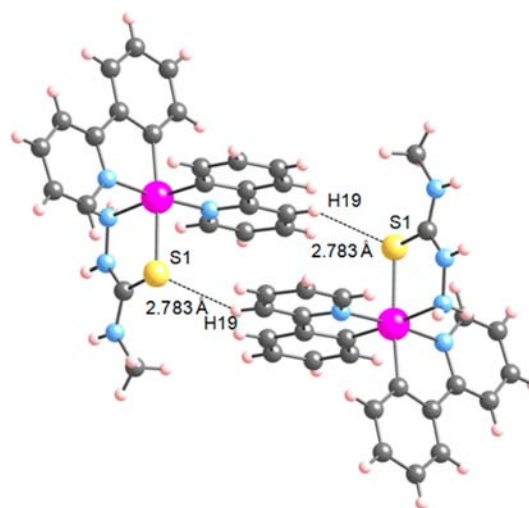


**Figure 2.** Schematic showing weak S···H–C contacts in 1.

**Table 1.** IC<sub>50</sub> (μM) and Resistance Factors for Cisplatin, and Compounds 1–3

complex	T47D 48 h	A2780 48 h	A2780 <sub>cisR</sub> 48 h (RF) <sup>a</sup>
1	15 ± 1	11 ± 1	9.27 ± 0.20 (0.84)
2	9.95 ± 0.04	4.93 ± 0.02	4.38 ± 0.19 (0.9)
3	9.93 ± 0.07	5.50 ± 0.07	5.71 ± 0.06 (1.04)
cisplatin	53 ± 3	1.54 ± 0.11	16 ± 1 (10.39)

<sup>a</sup>The numbers in parentheses are the resistance factors RF (IC<sub>50</sub> resistant/IC<sub>50</sub> sensitive).

resistant) and epithelial ovarian carcinoma cells A2780 and A2780<sub>cisR</sub> (acquired resistance to cisplatin). Because of low aqueous solubility of 1–3, the test compounds were dissolved in DMSO first and then serially diluted in complete culture medium such that the effective DMSO content did not exceed 1%. Complexes 1–3 were more active than cisplatin in T47D (about 5-fold).

On the other hand, A2780<sub>cisR</sub> encompasses all of the known major mechanisms of resistance to cisplatin: reduced drug transport,<sup>31</sup> enhanced DNA repair/tolerance,<sup>32</sup> and elevated GSH levels.<sup>33</sup> The ability of complexes 1–3 to circumvent cisplatin acquired resistance was determined from the resistance factor (RF) defined as the ratio of IC<sub>50</sub> resistant line to IC<sub>50</sub> parent line, very low RF values being observed at 48 h (RF = 0.9–1.0, Table 1), an RF of <2 was considered to denote noncross-resistance.<sup>34</sup> The IC<sub>50</sub> value for the free thiosemicarbazide ligands was higher than 100 μM in all the cancer cell lines studied.

The stability of the cytotoxic compounds 1–3 has been tested in a mixture DMSO-d<sub>6</sub>/D<sub>2</sub>O (1:1) in the presence of an excess of NaCl (100 mM) by <sup>1</sup>H NMR, remaining unaltered after 24 h in solution at 37 °C.

**Iridium Cellular Accumulation Studies.** We have determined the Ir accumulation in a T47D cell line after 48 h continuous exposure with 20 μM of complexes 1–3 (Table 2), showing higher values (about 10 times) than that corresponding to cisplatin. A direct relationship between metal accumulation and activity has not been described yet,<sup>35,36</sup> and it is not clearly observed in our measurements.

**Biological Assays: Gel Electrophoresis of Compound–pBR322 Complexes.** The influence of the compounds on the tertiary structure of DNA was determined by their ability to

**Table 2. Cellular Accumulation of Iridium Compounds 1–3 and Cisplatin in Human Breast Carcinoma T47D Cells**

compound	cellular accumulation <sup>a</sup> (pmol Ir/10 <sup>6</sup> cells) 48 h
1	22.376 ± 0.045
2	24.174 ± 0.246
3	18.518 ± 0.087
cisplatin	2.231 ± 0.005

<sup>a</sup>Drug-treatment period with 20 μM Ir complexes.

modify the electrophoretic mobility of the covalently closed circular (ccc) and open (oc) forms of pBR322 plasmid DNA. The compounds 1–3 were incubated at the molar ratio  $r_i = 0.50$  with pBR322 plasmid DNA at 37 °C for 24 h. Representative gel obtained for the new compounds 1–3 are shown in Supporting Information, Figure S2. The behavior of the gel electrophoretic mobility of both forms, ccc and oc, of pBR322 plasmid and DNA:cisplatin adducts is consistent with previous reports.<sup>37</sup> Noteworthy, the free thiosemicarbazide ligands and their iridium(III) derivatives 1–3 do not seem to cause important conformational changes of DNA.

**Competitive Binding Experiments.** To further investigate the binding mode between the new metal complexes and DNA, fluorescence competition experiments with ethidium bromide (EB) and Hoechst 33258 were employed. EB is a planar cationic dye well-known to intercalate into the DNA helix. While EB is only weakly fluorescent, the EB–DNA adduct is a strong emitter on excitation near 520 nm. Quenching of the fluorescence may be used to determine the extent of the binding between the quencher (1–3) and DNA. One reason for the quenching is the reduction in the number of binding sites on the DNA that is available to the EB presumably because of competition with complexes which is nonemissive under the experimental conditions.<sup>38,39</sup> As seen in Figure 3

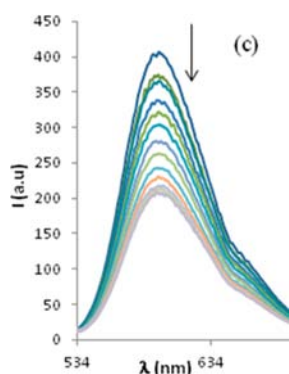


**Figure 3.** Fluorescence spectra of the EB-bound ct-DNA in aqueous buffer in the absence and presence of increasing amounts of complex 3.  $\lambda_{\text{ex}} = 520$  nm,  $[\text{EB}] = 0.33$  μM,  $[\text{DNA}] = 10$  μM,  $[\text{complexes}]$  (μM): 0–70 in 5 μM increments.  $T = 298$  K.

complex 3 causes a moderate decrease in the fluorescence at 602 nm as the amount of 3 is increased. For complexes 1 and 2 decrease in the fluorescence at 602 nm is smaller (Supporting Information, Figure S3).

To quantitatively assess the magnitude of this interaction between the complexes and DNA, the Stern–Volmer eq 1 is used.

$$F_0/F = 1 + K_{\text{SV}}[Q] \quad (1)$$

Here  $F_0$  and  $F$  are the fluorescence intensity of the EB–DNA adduct before and after the addition of the complex,  $K_{\text{SV}}$  is the Stern–Volmer quenching constant, and  $[Q]$  is the concentration of the corresponding metal complex. The good linearity of the Stern–Volmer plots (Supporting Information, Figure S4) suggests a singular mode of quenching. The values for the  $K_{\text{SV}}$  are given in Table 3. These values are in the  $10^3$ – $10^4$  M<sup>-1</sup>

**Table 3. Quenching and Binding Parameters for the Interaction of 1–3 with ct-DNA**

compound	$10^{-3}K_{\text{SV}}$ (M <sup>-1</sup> )	$10^{-3}K_{\text{app}}$ (M <sup>-1</sup> )
1	5.47	3.33
2	5.49	4.05
3	17.5	7.72

range which makes them very weak intercalators. The apparent binding constant for complexes was calculated using the eq 2.

$$K_{\text{app}} = K_{\text{EB}}[\text{EB}]/[\text{Q}]_{50\%} \quad (2)$$

Here  $K_{\text{EB}} = 1.2 \times 10^6$  M<sup>-1</sup>.<sup>40</sup>  $K_{\text{EB}}$  is the binding constant of EB to DNA and  $[\text{Q}]_{50\%}$  is the concentration of 1–3 at 50% of the initial fluorescence. These  $K_{\text{app}}$  values are also given in Table 3 and are on the same order of magnitude as the  $K_{\text{SV}}$  values.

Furthermore, we carried out a similar competition experiment using Hoechst 33258. This dye binds to DNA in two concentration dependent ways. The first type of binding occurs in the minor groove at low dye-to DNA ratios.<sup>41,42</sup> The fluorescence yield of Hoechst 33258 increases significantly in presence of DNA.<sup>43</sup> The displacement of bound Hoechst 33258 from its binding site on ct-DNA is implicated from a decrease in its fluorescence intensity on addition of the complexes. When the complexes are added to Hoechst–DNA solution we observed a decrease (~14% for 1 and ~55% for 2 and ~81% for 3, respectively) in the fluorescence (Figure 4). This suggests that especially complexes 2 and 3 are capable of binding in the minor groove of DNA.

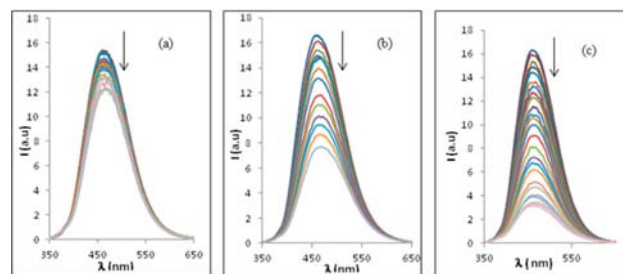


**Figure 4.** Fluorescence spectra of the Hoechst-bound ct-DNA in aqueous buffer in the absence and presence of increasing amounts of complexes 1 (a), 2 (b), and 3 (c).  $\lambda_{\text{ex}} = 338$  nm,  $[\text{Hoechst}] = 2$  μM,  $[\text{DNA}] = 20$  μM,  $[\text{complexes}]$  (μM): 0–30 in 2.5 μM increments.  $T = 298$  K.

**Reactions of the Iridium(III) Complexes 1–3 with 9-Ethylguanine.** The reactions were carried out in D<sub>2</sub>O and DMSO-d<sub>6</sub> (1:1) as solvents. The model nucleobase 9-EtG was incubated with the corresponding complex in a ratio 5:1 at 37 °C. After 24 h no reaction of 1–3 with 9-ethylguanine by <sup>1</sup>H NMR was observed in the assayed conditions.

**In Vitro Biological Evaluation for Activity against Bovine Cathepsin B.** Cathepsin B (cat B) is an abundant and ubiquitously expressed cysteine peptidase of the papain family.

Increased expression and secretion of cat B have been shown to be causally involved in immigration and invasion of numerous human and experimental tumors<sup>44</sup> and is a possible therapeutic target for the control of tumor progression, and in this respect, it is not surprising that the use of cat B inhibitors reduces both tumor cell mobility and invasiveness in vitro.<sup>45</sup> Recently, some metal complexes were shown to be effective inhibitors of cat B.<sup>46</sup> Complexes 1–3 were evaluated for activity against bovine cat B, and the in vitro  $IC_{50}$  data are reported in Table 4. These

**Table 4. In Vitro Biological Data for 1–3 against Bovine Cat B**

compound	$IC_{50}/\mu M$ vs cat B
1	$7.9 \pm 1.3$
2	$6.1 \pm 1.4$
3	$17.7 \pm 3.3$

values indicate that 1 and 2 are good cathepsin B inhibitors, showing values in the same order of magnitude than RAPTAC.<sup>46</sup> Figure 5 shows the reduction of enzyme activity as a

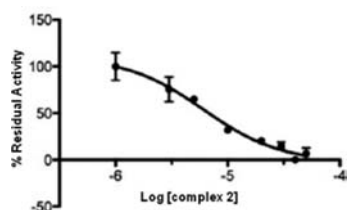


**Figure 5.** Cat B activity inhibition curves for complex 2.

function of inhibitor concentration for compound 2 displayed moderate cat B activity possibly because of the steric hindrance of the larger arene ring, which might decrease the accessibility of the iridium center in the active site.<sup>46</sup>

In addition, the cysteine reactivation properties were evaluated for 2 to characterize the reversibility of inhibition (Figure 6). It was found that the addition of 1 mM cysteine

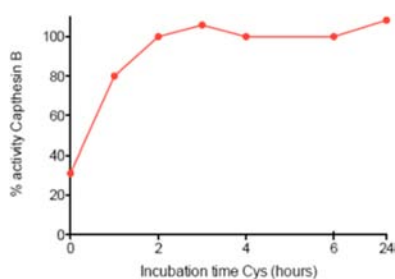


**Figure 6.** Cysteine reactivation of cat B data inhibited by 12  $\mu M$  of 2.

results in full recovery of activity within 2 h. These data support the hypothesis that loss of enzyme activity is due to specific interactions of the compound with the cat B active site instead of metal complex induced enzyme denaturing.<sup>47</sup>

**Reaction with HSA.** The interaction of Ir(III) complexes with HSA was monitored by studying the quenching of the fluorescence of HSA with increasing concentration of Ir(III) complexes. No correction for inner filter effect was applied since the Ir(III) complexes represented very low absorbance (less than 0.04) at the excitation and emission wavelengths, Supporting Information, Figure S5.<sup>48</sup> HSA has a well-known

structure consisting of a single polypeptide chain. Of the amino acid residues in the chain, the single tryptophan (Trp 214) is responsible for the majority of the intrinsic fluorescence of the protein. HSA has a strong fluorescence emission with a peak near 350 nm upon excitation at 295 nm. The emission is sensitive to the changes in the local environment of the tryptophan and so can be attenuated by binding of a small molecule at or near this residue. Thus, the emission spectra of HSA in the presence of different concentrations of Ir(III) complexes were recorded in the wavelength range 300–580 nm by exciting the protein at 295 nm. As seen in Figure 7, in all cases the fluorescence intensities of the protein are decreased regularly with increasing concentration of the probe compounds, indicating the binding of complex to the protein. A decrease in the fluorescence intensity of HSA at 348 nm accompanies the appearance of one peak at about 490 nm, which can be attributed to the fluorescence spectra of the Ir(III) complexes bound to the protein.

Furthermore, the fluorescence quenching mechanism can be described again by the Stern–Volmer eq 1. For a homogeneously emitting solution eq 1 predicts a linear plot of  $F_0/F$  vs  $[Q]$ , but for many systems the plots have been found to curve upward. This is the case for the new complexes herein reported (Supporting Information, Figure S6). It sometimes has been proposed as explanation that in addition to the dynamic quenching which governs the Stern–Volmer plot, a second mechanism, static quenching occurs.<sup>49,50</sup>

A common method to distinguish between static and dynamic quenching is by careful examination of the absorption spectra of the HSA in the presence of the metal complexes.

Figure 8 shows the absorption spectra of HSA before and after the addition of Ir(III) complexes. The influence of the absorbance of Ir(III) complexes were eliminated by adding in the reference cells the solutions of Ir complexes of the same concentrations as in the sample solution. As can be seen, the protein possess two absorption peaks at 206 and 279 nm, where that at 206 nm represents the content of  $\alpha$ -helix in the protein and the weak absorption peak at 279 nm arises from the phenyl rings in Trp (tryptophan), Tyr (tyrosine), and Phe (phenylalanine) residues. A dramatic decrease in the 206 nm absorbance peak of the protein is observed upon addition of complexes to the protein. This can be attributed to the induced perturbation of  $\alpha$ -helix of protein by a specific interaction with the ligands. Furthermore, an obvious red shift in the position of the absorbance peak at 206 nm (i.e., 228 nm for complex 1, 229 nm for complex 2, and 230 nm for complex 3) could also be observed with the addition of complexes. Meanwhile, a subtle change in the intensity and a blue shift in the position of the absorbance peak at 279 nm (i.e., 277 nm for complex 1, 266 nm for complex 2, and 273 nm for complex 3) could also be observed indicating that more aromatic acid residues were extended into the aqueous environment.<sup>51,52</sup> Trp-214 in HSA, which are originally buried in a hydrophobic pocket, were exposed to an aqueous milieu to a certain degree.

This result indicated that the microenvironment of the three aromatic acid residues was altered and the tertiary structure of HSA was destroyed. Overall, the changes in the absorbance spectra for HSA + complexes show that the interaction between Ir(III) complexes and HSA was mainly a static quenching process.

For a static quenching process, the association constant ( $K_A$ ) and the number of binding sites ( $n$ ) can be calculated using eq 3.

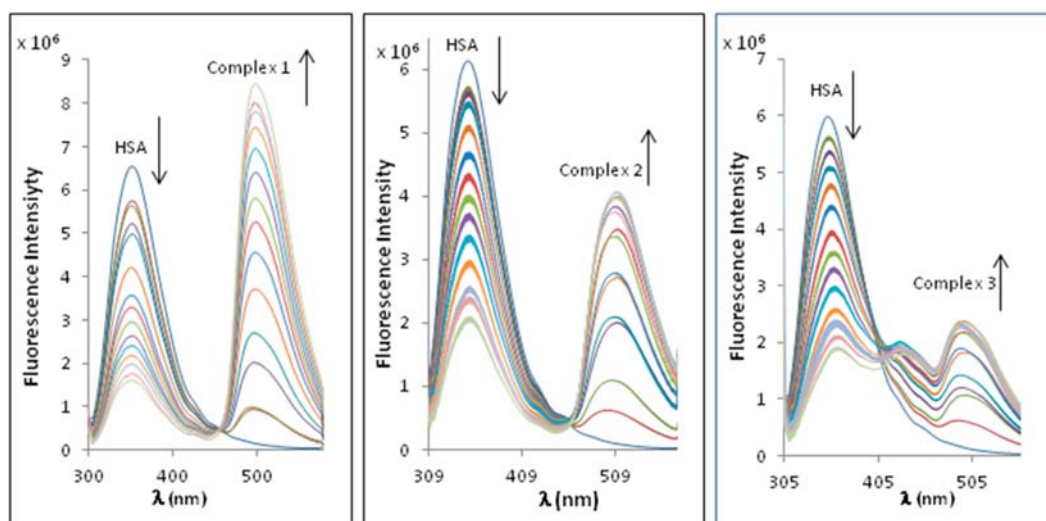


**Figure 7.** Emission spectra of the HSA in presence of increasing amounts of complexes 1–3.  $\lambda_{\text{ex}} = 295$  nm,  $[\text{HSA}] = 5.4 \mu\text{M}$ , and  $[\text{complexes}]$ : 0–35  $\mu\text{M}$  (top-to-bottom in 2.7  $\mu\text{M}$  increments). Temperature = 296 K and pH = 7.4.

$$\log \frac{F_0 - F}{F} = n \log K_A - n \log \left\{ \frac{1}{[\text{Q}_t] - (F_0 - F)[\text{P}_t]/F_0} \right\} \quad (3)$$

Here  $F_0$  and  $F$  are the fluorescence intensities in the absence and presence of complexes, respectively;  $[\text{Q}_t]$  and  $[\text{P}_t]$  are the total concentrations of complexes and HSA, respectively.

Supporting Information, Figure S7 shows the plots of  $\log (F_0 - F)/F$  versus  $\log \{1/([\text{Q}_t] - (F_0 - F)[\text{P}_t]/F_0)\}$  for the interaction between HSA and complexes 1–3.  $K_A$  and  $n$  obtained from the plots and  $K_{\text{sv}}$  are listed in Table 5.

The binding constant is on the order of  $10^4 \text{ M}^{-1}$  for all complexes, indicating strong binding to the protein, and the number of binding sites in HSA approximates to 2 for complexes 2 and 3, indicating that two sites in HSA are reactive to both complexes. For the compound 1 a single site in HSA is reactive to complex.

**Site-Selective Binding of Ir Complexes on HSA.** To identify the binding site location of Ir(III) complexes on the region of HSA, competitive binding experiments were carried out using warfarin, a characteristic marker for site I (subdomain IIA), and ibuprofen as one for site II (subdomain IIIA).<sup>48</sup> Thus information about complex 2 binding site can be obtained by monitoring the changes in the fluorescence spectra of Ir(III) complex bound to HSA. The weak fluorescence intensity of warfarin is enhanced upon binding with HSA because of its interaction with Trp 214 in HSA when excited at 320 nm. The fluorescence intensity of warfarin, in its bound state to HSA, decreases if a second ligand competes for the site occupied by it. Thus, the accessibility of Trp 214 in HSA by ligands can be confirmed by monitoring the displacement of warfarin by 2 in the HSA–warfarin complex. As shown in Supporting Information, Figure S8, a decrease in the emission intensity of HSA–warfarin (in the wavelength region of 348–450 nm, excited at 320 nm) is observed when 2 is added. The quenching of warfarin bound to protein upon addition of 2 reflects a reduction in the warfarin binding capacity at the binding site of HSA and preferential accessibility of Trp 214 in HSA by 2. Therefore it is very likely that the 2 binding occurs at the warfarin site I.

To investigate if complex 2 can also bind to the site II of albumin, an ibuprofen competitive experiment was conducted. Ibuprofen was gradually added to the solution containing equimolar concentrations of HSA and 2, and the change in fluorescence intensity of 2 ( $\lambda_{\text{ex}} = 320$  nm,  $\lambda_{\text{em}} = 520$  nm) was monitored (Supporting Information, Figure S9). The binding constant of ibuprofen to HSA is  $3.6 \times 10^6 \text{ M}^{-1}$ , which is higher than that of complex 2. So, if 2 binds to site II of albumin, it would be substituted by ibuprofen. The unbound Ir complex has a weaker fluorescence emission than the albumin-bound complex. Thus a decrease in the fluorescence intensity of 2 upon addition of ibuprofen is expected if 2 binds to site II of albumin. However, it was found that the fluorescence intensities of albumin-bound 2 complex increases upon addition of ibuprofen. Therefore, this seems to indicate that 2 is not able to bind to the site II of albumin.

## CONCLUSIONS

Three new organometallic iridium(III) thiosemicarbazide complexes  $[\text{Ir}(\text{N}-\text{C})_2(\text{N}-\text{S})]\text{Cl}$  ( $\text{HN}-\text{C} = 2$ -phenylpyridine) 1–3 have been prepared, where the thiosemicarbazide ligand binds the iridium atom as N,S-chelate, as confirmed for 1 by X-ray diffraction. 1–3 were more cytotoxic than cisplatin in T47D human breast cancer cell line (about 5-fold). Especially noteworthy is the very low resistance factor (RF) of 2 and 3 at 48 h (RF = 0.9 and 1.1, respectively) against an A2780 cell line which has acquired resistance to cisplatin indicating efficient circumvention of cisplatin resistance. Ir accumulation in T47D cell line after 48 h continuous exposure for complexes 1–3 are higher than that corresponding to cisplatin (about 10 times). Complexes 1 and 2 are good cathepsin B inhibitors (an enzyme implicated in a number of cancer related events), being the enzyme reactivated by cysteine. The binding constant toward HSA is on the order of  $10^4 \text{ M}^{-1}$  at 296 K for all complexes, indicating strong binding to the protein, and the number of binding sites in HSA approximates to 2 for complexes 2 and 3, indicating that two sites in HSA are reactive to both complexes, binding occurring at the warfarin site I as shown for 2. For the compound 1 a single site in HSA is reactive to complex. Furthermore, as shown by Hoechst 33258 displacement experiments, 2 and 3 are able to bind to DNA in

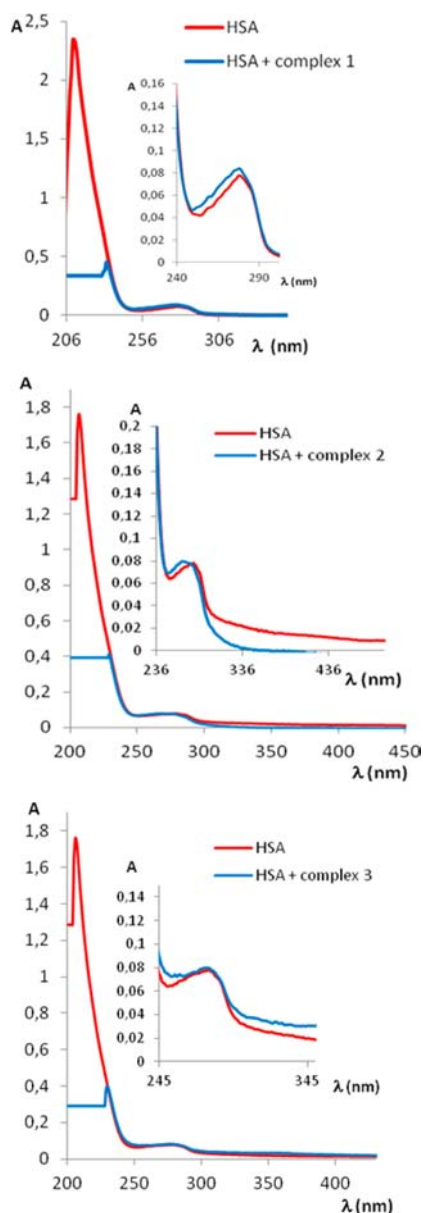


**Figure 8.** Absorption spectra of HSA = ( $10^{-6}$  M) (red), HSA + complex 1, 2, or 3 =  $10^{-6}$  M and  $10^{-5}$  M respectively (blue).

**Table 5. Quenching and Binding Parameters for the Interaction of Complexes with HSA**

	$T$ (K)	$10^{-4} K_{sv}^a$ ( $M^{-1}$ )	$R^2$	$10^{-4} K_A$ ( $M^{-1}$ )	$n$
complex 1	296	9.35	0.993	5.34	1.32
complex 2	296	4.24	0.989	3.48	2.18
complex 3	296	4.26	0.980	3.92	1.91

<sup>a</sup>Calculated using only the data in the linear range.

the minor groove. No reaction of 1–3 with 9-EtG was observed by  $^1H$  NMR in the assayed conditions.

## EXPERIMENTAL SECTION

**Instrumental Measurements.** The C, H, N, and S analyses were performed with a Carlo Erba model EA 1108 microanalyzer. Decomposition temperatures were determined with a SDT 2960 simultaneous DSC-TGA of TA Instruments at a heating rate of  $5\text{ }^\circ\text{C min}^{-1}$  and the solid samples under nitrogen flow ( $100\text{ mL min}^{-1}$ ). Infrared spectra were recorded on a Perkin-Elmer 100 FT-IR

spectrometer using KBr pellets. The  $^1H$  and  $^{13}C$  NMR spectra were recorded on a Bruker AC 300E or Bruker AV 400 spectrometer, using SiMe<sub>4</sub> as standard. ESI mass (positive mode) analyses were performed on a HPLC/MS TOF 6220. UV/vis spectroscopy was carried out on a Perkin-Elmer Lambda 750 S spectrometer with operating software. Fluorescence measurements were carried out with a Perkin-Elmer LS 55 50 Hz Fluorescence Spectrometer.

**Materials.** Solvents were dried by the usual methods. The starting complex  $[Ir_2(N-C)_4Cl_2]$  (HN-C = Hppy) was prepared by a procedure described elsewhere.<sup>53</sup> The thiosemicarbazide ligands were synthesized by using procedures adapted from the literature.<sup>54,55</sup> Sodium salt of calf thymus DNA, ethidium bromide (EB), Hoechst 33258, serumalbumin (HSA) were obtained from Sigma-Aldrich (Madrid, Spain); pBR322 plasmid DNA used in the studies were obtained from Boehringer-Mannheim (Mannheim, Germany).

**Synthesis of Cyclometalated Iridium(III) Complexes.** A mixture of  $[Ir_2(N-C)_4Cl_2]$  (100 mg, 0.145 mmol) and the corresponding thiosemicarbazide (0.290 mmol) in 20 mL of EtOH/CH<sub>2</sub>Cl<sub>2</sub> (3:1, v/v) was stirred for 72 h at room temperature to yield a solution, which was partially evaporated under vacuum, and ethyl ether and hexane was added to precipitate the complexes as yellow solids, which were collected by filtration and air-dried.

**Complex 1.** Yield: 62%. Anal. Calcd for 1 C<sub>24</sub>H<sub>23</sub>N<sub>5</sub>ClIr: C, 44.96; H, 3.62; N, 10.92; S, 5.00. Found: C, 44.57; H, 3.89; N, 10.76; S, 5.01. Mp: 253 °C (dec). IR (cm<sup>-1</sup>):  $\nu(NH_2, NH)$  3404, 3205, 3039;  $\nu(C=N)$  1580;  $\nu(C=S)$  756.  $^1H$  NMR (300 MHz, DMSO-d<sub>6</sub>, TMS): 10.87 (m, 1 H, NH), 9.24 (m, 1 H ppy), 8.84 (m, 1H, NHCH<sub>3</sub>), 8.73 (m, 1 H ppy), 8.46 (m, 2H, NH<sub>2</sub>), 8.16 (m, 2H ppy), 7.97 (m, 2H ppy), 7.73 (m, 2 H ppy), 7.43 (m, 2 H ppy), 6.73 (m, 4 H ppy), 6.21 (m, 1H ppy), 6.06 (m, 1 H ppy), 2.88 (m, 3H, CH<sub>3</sub>). Positive-ion ESI mass spectra ion cluster (DMSO) at  $m/z$  604  $\{[Ir(ppy)_2(\text{methylthiosemicarbazide})]^+\}^+$ .

**Complex 2.** Yield: 65%. Anal. Calcd for 2 C<sub>28</sub>H<sub>25</sub>N<sub>5</sub>ClIr: C, 48.65; H, 3.65; N, 10.13; S, 4.64. Found: C, 48.53; H, 3.87; N, 9.85; S, 4.63. Mp: 237 °C (dec). IR (cm<sup>-1</sup>):  $\nu(NH_2, NH)$  3412, 3144, 3035;  $\nu(C=N)$  1496;  $\nu(C=S)$  756.  $^1H$  NMR (300 MHz, DMSO-d<sub>6</sub>, TMS): 11.27 (m, 2H, NH<sub>2</sub>), 9.25 (d, 1H ppy,  $J = 6$  Hz), 8.78 (d, 1H ppy,  $J = 6$  Hz), 8.66 (m, 1H, NH), 8.19 (m, 2H ppy), 7.99 (m, 3H, 2H ppy + 1H NH), 7.79 (d, 1H ppy,  $J = 6$  Hz), 7.71 (d, 1H ppy,  $J = 6$  Hz), 7.50–7.32 (m, 6H, 2H<sub>0</sub> + 2H<sub>m</sub> phenylthiosemicarbazide + 2H ppy), 7.19 (m, 1H, H<sub>p</sub> phenylthiosemicarbazide), 6.89 (m, 1H ppy), 6.77 (m, 2H ppy), 6.23 (m, 1H ppy), 6.20 (d, 1H ppy,  $J = 6$  Hz), 6.05 (d, 1H ppy,  $J = 6$  Hz). Positive-ion ESI mass spectra ion cluster (DMSO) at  $m/z$  656  $\{[Ir(ppy)_2(\text{phenylthiosemicarbazide})]^+\}^+$ .

**Complex 3.** Yield: 57%. Anal. Calcd for 3 C<sub>33</sub>H<sub>27</sub>N<sub>5</sub>ClIr: C, 52.61; H, 3.61; N, 9.30; S, 4.26. Found: C, 52.42; H, 3.85; N, 9.12; S, 4.35. Mp: 223 °C (dec). IR (cm<sup>-1</sup>):  $\nu(NH_2, NH)$  3434, 3159, 3040;  $\nu(C=N)$  1550;  $\nu(C=S)$  756.  $^1H$  NMR (400 MHz, DMSO-d<sub>6</sub>, TMS): 11.07 (s, 1H, NH), 9.24 (d, 1 H ppy,  $J = 7$  Hz), 8.82 (d, 1 H, ppy,  $J = 7$  Hz), 8.62 (d, 1 H, NHNH<sub>2</sub>), 8.20 (d, 1 H ppy,  $J = 7$  Hz), 8.15 (d, 1 H ppy,  $J = 7$  Hz), 8.04 (m, 4 H ppy), 7.91 (m, 2 H, NHNH<sub>2</sub>), 7.78 (d, 1H ppy,  $J = 7$  Hz), 7.73 (m, 1 H naphthyl thiosemicarbazide), 7.66 (d, 1 H ppy,  $J = 7$  Hz), 7.6 (m, 3 H naphthylthiosemicarbazide), 7.5 (m, 3 H ppy), 6.87 (m, 1 H ppy), 6.7 (m, 2 H ppy), 6.6 (m, 1 H ppy), 6.22 (d, 1 H ppy,  $J = 7$  Hz), 5.97 (d, 1 H ppy,  $J = 7$  Hz). Positive-ion ESI mass spectra ion cluster (DMSO) at  $m/z$  716  $\{[Ir(ppy)_2(\text{naphthylthiosemicarbazide})]^+\}^+$ .

**Reactions of the Iridium(III) Complexes with 9-Ethylguanine Followed by  $^1H$  NMR.** The reaction was carried out in an NMR tube containing D<sub>2</sub>O and DMSO-d<sub>6</sub> (1:1 in volume) as solvents. 9-Ethylguanine was incubated with the complexes in a ratio 5:1 in the above solvents mixture at 37 °C. The concentration of complexes was 1.0 mM.

**X-ray Crystal Structure Analysis.** Suitable crystals of 1 were grown from dichloromethane/hexane. The crystal and molecular structure of 1 have been determined by X-ray diffraction studies (Table 6). Crystals were mounted on glass fibers and transferred to the cold gas stream of the diffractometer Bruker Smart APEX. Data were recorded with Mo K $\alpha$  radiation ( $\lambda = 0.71073\text{ \AA}$ ) in  $\omega$  scan mode. Absorption correction for the compound was based on multiscans.

Table 6. Crystal Structure Determination Details of 1

1	
chemical formula	C <sub>24</sub> H <sub>23</sub> ClIrN <sub>5</sub> S
fw [g/mol]	641.18
cryst system	monoclinic
a [Å]	15.5488(12)
b [Å]	9.3007(7)
c [Å]	20.6588(17)
β [deg]	90.836(2)
V [Å <sup>3</sup> ]	4049.4(3)
temp (K)	100(2) K
space group	P2(1)/n
Z	4
μ [mm <sup>-1</sup> ]	4.646
reflcs collcd	19904
indpdnt reflcs	6549
R(int)	0.0304
R1 [I > 2σ(I)] <sup>a</sup>	0.0269
wR <sub>2</sub> (all data) <sup>b</sup>	0.0634

<sup>a</sup>R1 =  $\sum ||F_o| - |F_c|| / \sum |F_o|$ , wR2 =  $[\sum [w(F_o^2 - F_c^2)^2] / \sum w(F_o^2)^2]^{0.5}$ .  
<sup>b</sup>w =  $1 / [\sigma^2(F_o^2) + (aP)^2 + bP]$ , where  $P = (2F_c^2 + F_o^2) / 3$ , and *a* and *b* are constants set by the program.

The structure was solved by direct method, and refined anisotropically on  $F^2$ .<sup>56</sup> The hydrogens at N were located in the Fourier difference maps and refined freely with DFIX. Methyl groups were refined using rigid groups, and other hydrogens were refined using a riding method.

**Special Features for 1.** The structure contains a poorly resolved region of residual electron density; this could not be adequately modeled and so was “removed” using the program SQUEEZE,<sup>57</sup> which is part of the PLATON<sup>58</sup> system. The void volume per cell was 888.6 Å<sup>3</sup>, with a void electron count per cell of 187. This additional solvent was NOT taken account of when calculating derived parameters such as the formula weight because the nature of the solvent was uncertain.

**Cell Line and Culture.** The T-47D human mammary adenocarcinoma cell line used in this study was grown in RPMI-1640 medium supplemented with 10% (v/v) fetal bovine serum (FBS) and 0.2 unit/mL bovine insulin in an atmosphere of 5% CO<sub>2</sub> at 37 °C. The human ovarian carcinoma cell lines (A2780 and A2780cisR) used in this study were grown in RPMI 1640 medium supplemented with 10% (v/v) fetal bovine serum (FBS) and 2 mM L-glutamine in an atmosphere of 5% CO<sub>2</sub> at 37 °C.

**Cytotoxicity Assay.** Cell proliferation was evaluated by assay of crystal violet. T-47D cells plated in 96-well sterile plates at a density of  $5 \times 10^3$  cells/well with 100 μL of medium and were then incubated for 48 h. After attachment to the culture surface the cells were incubated with various concentrations of the compounds tested freshly dissolved in DMSO and diluted in the culture medium (DMSO final concentration 1%) for 48 h at 37 °C. The cells were fixed by adding 10 μL of 11% glutaraldehyde. The plates were stirred for 15 min at room temperature and then washed three-four times with distilled water. The cells were stained with 100 μL of 1% crystal violet. The plates were stirred for 15 min and then washed three-four times with distilled water and dried. A 100 μL portion of 10% acetic acid was added, and it was stirred for 15 min at room temperature.

Absorbance was measured at 595 nm in a Tecan Ultra Evolution spectrophotometer.

The effects of complexes were expressed as corrected percentage inhibition values according to the following equation,

$$(\%) \text{ inhibition} = [1 - (T/C)] \times 100$$

where *T* is the mean absorbance of the treated cells and *C* the mean absorbance in the controls.

The inhibitory potential of compounds was measured by calculating concentration–percentage inhibition curves; these curves were adjusted to the following equation:

$$E = E_{\max} / [1 + (IC_{50}/C)^n]$$

where *E* is the percentage inhibition observed,  $E_{\max}$  is the maximal effect,  $IC_{50}$  is the concentration that inhibits 50% of maximal growth, *C* is the concentration of compounds tested, and *n* is the slope of the semilogarithmic dose–response sigmoid curves. This nonlinear fitting was performed using GraphPad Prism 2.01, 1996 software (GraphPad Software Inc.).

For comparison purposes, the cytotoxicity of cisplatin was evaluated under the same experimental conditions. All compounds were tested in two independent studies with triplicate points. The in vitro studies were performed in the USEF platform of the University of Santiago de Compostela (Spain).

**Cellular Iridium Complexes Accumulation.** T-47D cells were plated in a 12-well cell culture plate at a density of 750000 cells/well and maintained at 37 °C in a 5% CO<sub>2</sub> atmosphere. Compounds to 20 μM were added to cells for 48 h, and after this time, cells were detached from the plate by using EDTA-trypsin. The cell suspension from each well was transferred to Eppendorf tubes and centrifuged at 400 g for 5 min at room temperature. The supernatant was discarded, and the pellet was suspended in a cell culture medium and washed by two additional centrifugations. The final pellet was resuspended in 0.5 mL of pure HNO<sub>3</sub> and diluted with 5 mL of Milli-Q water for ICP-MS analysis. A Varian 820-MS inductively coupled plasma-mass spectrometer was used to determine Ir concentration. Samples were introduced via a concentric glass nebulizer with a free aspiration rate of 1 mL/min, a Peltier-cooled double pass glass spray chamber, and a quartz torch. A peristaltic pump carried samples from a SPS3 autosampler (Varian) to the nebulizer. Ir standards were prepared by serial dilution of a solution containing 1000 mg/L of Ir in 5% HCl (Trace Cert. Fluka). A nine-point calibration curve was made over a concentration range of 0.2–100 μg/L of Ir.

<sup>193</sup>Ir and <sup>191</sup>Ir were monitored, and <sup>159</sup>Tb was used as the internal standard. Data acquisition was done using peak hopping with a dwell time of 30 ms, 60 scans/replicate, and three replicates per sample from two independent experiments.

**Electrophoretic Mobility Study.** pBR322 plasmid DNA of 0.25 μg/μL concentration was used for the experiments. Four microliters of charge maker (Lambda-pUC Mix marker, 4) were added to aliquots parts of 20 μL of the drug–DNA complex. The iridium complexes were incubated at the molar ratio  $r_1 = 0.50$  with pBR322 plasmid DNA at 37 °C for 24 h. The mixtures underwent electrophoresis in agarose gel 1% in 1 × TBE buffer (45 mM Tris-borate, 1 mM EDTA, pH 8.0) for 5 h at 30 V. Gel was subsequently stained in the same buffer containing ethidium bromide (1 μg/mL) for 20 min. The DNA bands were visualized with an AlphaImager EC (Alpha Innotech).

**Ethidium Bromide and Hoechst 33258 Displacement Experiments.** In the ethidium bromide (EB) fluorescence displacement experiment 3 mL of a solution, that is, 10 μM DNA and 0.33 μM EB (saturated binding levels<sup>59</sup>), in Tris buffer was titrated with aliquots of a concentrated solution of the complex producing solutions with varied mole ratios of complex to ct-DNA. After each addition the solution was stirred at the appropriate temperature for 5 min before measurement. The fluorescence spectra of the solution were obtained by exciting at 520 nm and measuring the emission spectra from 530–700 nm using 5 nm slits. The procedure was the same for the Hoechst 33258 reactions using the following conditions: working solutions were 20 μM DNA and 2 μM Hoechst 33258;  $\lambda_{\text{ex}} = 338$  nm and  $\lambda_{\text{em}} = 350$ –650 nm (with  $\lambda_{\text{max}} \sim 600$  nm).

**Cathepsin B Inhibition Assay.** Crude bovine spleen cat B was purchased from Sigma (C6286) and used without further purification. The colorimetric cat B assay was performed in 100 mM sodium phosphate, 1 mM EDTA, 0.025% polyoxyethylene (23) lauryl ether (BRJ), pH = 6 using Z-L-Lys-ONp hydrochloride (Sigma C3637) as substrate. For the enzyme to be catalytically functional, the active site cysteine needs to be in a reduced form. Therefore, before using, cat B was prerduced with dithiothreitol (DTT) to ensure that the majority

of the enzyme is in a catalytically active form. Thus, cat B was activated, before dilution, in the presence of excess DTT for 1 h at 30 °C.

$IC_{50}$  determinations were performed in duplicate using a fixed enzyme concentration of 1  $\mu$ M, and a fixed substrate concentration of 0.08 mM. Inhibitor concentrations ranged from 1  $\mu$ M to 50  $\mu$ M. The enzyme and inhibitor were co-incubated at 25 °C over a period of 24 h prior to the addition of substrate. Activity was measured over 1 min at 326 nm.

Cysteine reactivation was evaluated using an inhibitor concentration corresponding to  $2 \times IC_{50}$ . The enzyme was preincubated with an excess of DTT (Sigma D0632) for 1 h at 30 °C. After the activation, the enzyme and the compound were incubated at 25 °C for 24 h. Then, 1 mM L-cysteine was added and incubated at different times 1, 2, 3, 4, 6, and 24 h at 25 °C. Following incubation, the substrate was added, and activity was assessed.

**Reaction with Human Serum Albumin (HSA). Procedures Fluorescence Quenching Studies.** The stock solutions of proteins ( $5.4 \times 10^{-6}$  mol L<sup>-1</sup>) were prepared by dissolving the solid HSA in 50 mM Tris-HCl, 100 mM NaCl buffer of pH 7.4 and stored at 0–4 °C in the dark for about a week. The concentrations of HSA were determined from optical density measurements, using the values of molar absorptivity of  $\epsilon_{278} = 36\,000$  M<sup>-1</sup> cm<sup>-1</sup>.<sup>48</sup>

Quantitative analyses of the interaction between Ir(III) complexes 1–3 and biomacromolecules were performed by fluorimetric titration. A 3.0 mL portion of aqueous solution of protein ( $5.4 \times 10^{-6}$  mol L<sup>-1</sup>) was titrated by successive additions of Ir(III) complexes solution (to give a final concentration of  $35 \times 10^{-6}$  mol L<sup>-1</sup>). Titrations were done manually by using a trace syringe. For every addition, the mixture solution was shaken and allowed to stand for 5 min at the corresponding temperature, and then the fluorescence intensities were measured with an excitation wavelength of 295 nm and emission wavelengths in the interval 300–550 nm. No correction for inner filter effect was applied since the Ir(III) complexes represented very low absorbance (less than 0.04) at the excitation and emission wavelengths, Supporting Information, Figure S7. The width of the excitation and emission slit was set to 5 nm.

**Site Marker Competitive Experiments.** Binding location studies between Ir(III) complex and HSA in the presence of two site markers (warfarin and ibuprofen) were measured using the fluorescence titration methods.

**Warfarin as Marker of Site I.** The displacement experiments were performed using the site probe warfarin by preparing equimolar mixtures of biomacromolecule and warfarin (each  $1 \times 10^{-6}$  mol L<sup>-1</sup>), which were then thoroughly mixed and equilibrated at room temperature for 1 h. A 3.0 mL portion of the solution was transferred to a cell, and then it was titrated by successive additions of complex 2 solution. After thorough mixing of the resultant solution at each titration step, the solutions were allowed to stand for 20 min. An excitation wavelength of 320 nm was selected. The width of the excitation and emission slit was set to 5 nm, and the emission fluorescence spectra were recorded in the wavelength range 340–600 nm.

**Ibuprofen as Marker of Site II.** Equimolar mixtures of protein and complex 2 ( $1 \times 10^{-6}$  mol L<sup>-1</sup>) were thoroughly mixed and allowed to equilibrate at room temperature for 1 h. A 3.0 mL portion of the solution was transferred to the spectrofluorimetric cell, and then ibuprofen was gradually added to this solution. The procedure was the same as that in the displacement experiments using the site probe warfarin.

## ■ ASSOCIATED CONTENT

### ● Supporting Information

Structures, energies and Cartesian coordinates for all computed compounds. This material is available free of charge via the Internet at <http://pubs.acs.org>.

## ■ AUTHOR INFORMATION

### Corresponding Author

\*E-mail: [jruiz@um.es](mailto:jruiz@um.es). Fax: +34 868 884148. Tel: +34 868 887455.

### Notes

The authors declare no competing financial interest.

## ■ ACKNOWLEDGMENTS

This work was supported by the Spanish *Ministerio de Economía y Competitividad* and FEDER (Project SAF2011-26611) and also by *Fundación Séneca-CARM* (Project 08666/PI/08).

## ■ REFERENCES

- (1) Jakupec, M. A.; Galanski, M.; Arion, V. B.; Hartinger, C. G.; Keppler, B. K. *Dalton Trans.* **2008**, 183–194.
- (2) Klein, A. V.; Hambley, T. W. *Chem. Rev.* **2009**, *109*, 4911–4920.
- (3) Jung, Y. W.; Lippard, S. J. *Chem. Rev.* **2007**, *107*, 1387–1407.
- (4) O'Dwyer, P. J.; Stevenson, J. P.; Johnson, S. W. In *Cisplatin. Chemistry and Biochemistry of a leading Anticancer Drug*; Lippert, B., Ed.; Wiley-VCH: Weinheim, Germany, 1999; p 3172.
- (5) Wang, D.; Lippard, S. J. *Nat. Rev. Drug Discovery* **2005**, *4*, 307–320.
- (6) Hannon, M. J. *Pure Appl. Chem.* **2007**, *79*, 2243–2261.
- (7) van Zutphen, S.; Reedijk, J. *Coord. Chem. Rev.* **2005**, *249*, 2845–2853.
- (8) Gasser, G.; Ott, I.; Metzler-Nolte, N. *J. Med. Chem.* **2011**, *54*, 3–25.
- (9) *Medicinal Organometallic Chemistry*, 1st ed.; Bruijninx, P. C. A.; Topics in Organometallic Chemistry 32; Jaouen, G., Metzler-Nolte, N., Eds.; Springer-Verlag: Heidelberg, Germany, 2010.
- (10) Suss-Fink, G. *Dalton Trans.* **2010**, *39*, 1673–1688.
- (11) Dyson, P. J.; Sava, G. *Dalton Trans.* **2006**, 1929–1933.
- (12) Sadler, P. J. *Curr. Opin. Chem. Biol.* **2008**, *12*, 197–206.
- (13) Bruijninx, P. C. A.; Sadler, P. J. In *Advances in Inorganic Chemistry*; van Eldik, R., Hubbard, C. D., Eds.; Academic Press: New York, 2009; Vol. 61, pp 1–62.
- (14) Liu, H.-K.; Sadler, P. J. *Acc. Chem. Res.* **2011**, *44*, 349–359.
- (15) Hartinger, C.; Dyson, P. J. *Chem. Soc. Rev.* **2009**, *38*, 391–401.
- (16) Ang, W. H.; Parker, L. J.; De Luca, A.; Juillerat-Jeanneret, L.; Morton, C. J.; Lo Bello, M.; Parker, M. W.; Dyson, P. J. *Angew. Chem., Int. Ed.* **2009**, *48*, 3854–3857.
- (17) Liu, Z.; Salassa, L.; Habtemariam, A.; Pizarro, A. M.; Clarkson, G. J.; Sadler, P. J. *Inorg. Chem.* **2011**, *50*, 5777–5783.
- (18) Liu, Z.; Habtemariam, A.; Pizarro, A. M.; Clarkson, G. J.; Sadler, P. J. *Organometallics* **2011**, *30*, 4702–4710.
- (19) Patra, M.; Gasser, G. *ChemBioChem* **2012**, *13*, 1232–1252.
- (20) Lau, J. S.-Y.; Lee, P.-K.; Tsang, K. H.-K.; Ng, C. H.-C.; Lam, Y.-W.; Cheng, S.-H.; Lo, K. K.-W. *Inorg. Chem.* **2009**, *48*, 708–718.
- (21) Blanck, S.; Cruchter, T.; Vultur, A.; Riedel, R.; Harms, K.; Herlyn, M.; Meggers, E. *Organometallics* **2011**, *30*, 4598–4606.
- (22) Ruiz, J.; Vicente, C.; de Haro, C.; Bautista, D. *Dalton Trans.* **2009**, 5071–5073.
- (23) Ruiz, J.; Vicente, C.; de Haro, C.; Espinosa, A. *Inorg. Chem.* **2011**, *50*, 2151–2158.
- (24) Ruiz, J.; Rodríguez, V.; Cutillas, N.; Espinosa, A.; Hannon, M. J. *Inorg. Chem.* **2011**, *50*, 9164–9171.
- (25) Ruiz, J.; Rodríguez, V.; Cutillas, N.; Espinosa, A.; Hannon, M. J. *J. Inorg. Biochem.* **2011**, *105*, 525–531.
- (26) Ruiz, J.; Rodríguez, V.; Cutillas, N.; Samper, K. G.; Capdevilla, M.; Palacios, O.; Espinosa, A. *Dalton Trans.* **2012**, *41*, 12847–12856.
- (27) Auffrant, A.; Barbieri, A.; Barigelletti, F.; Lacour, J.; Mobian, P.; Collin, J. P.; Sauvage, J. P.; Ventura, B. *Inorg. Chem.* **2007**, *46*, 6911–6919.
- (28) Neve, F.; Crispini, A.; Campagna, S.; Serroni, S. *Inorg. Chem.* **1999**, *38*, 2250–2258.

- (29) Lamansky, S.; Djurovich, P.; Murphy, D.; Abdel-Razzaq, F.; Kwong, R.; Tsyba, I.; Bortz, M.; Mui, B.; Bau, R.; Thompson, M. E. *Inorg. Chem.* **2001**, *40*, 1704–1711.
- (30) Andreiadis, E. S.; Imbert, D.; Pécaut, J.; Calborean, A.; Ciofini, I.; Adamo, C.; Demadrille, R.; Mazzanti, M. *Inorg. Chem.* **2011**, *50*, 8197–8206.
- (31) Loh, S. Y.; Mistry, P.; Kelland, L. R.; Abel, G.; Harrap, K. R. *Brit. J. Cancer.* **1992**, *66*, 1109–1115.
- (32) Goddard, P. M.; Orr, R. M.; Valenti, M. R.; Barnard, C. F.; Murrer, B. A.; Kelland, L. R.; Harrap, K. R. *Anticancer Res.* **1996**, *16*, 33–38.
- (33) Behrens, B. C.; Hamilton, T. C.; Masuda, H.; Grotzinger, K. R.; Whang-Peng, J.; Louie, K. G.; Knutsen, T.; McKoy, W. M.; Young, R. C.; Ozols, R. F. *Cancer Res.* **1987**, *47*, 414–418.
- (34) Kelland, L. R.; Barnard, C. F. J.; Mellish, K. J.; Jones, M.; Goddard, P. M.; Valenti, M.; Bryant, A.; Murrer, B. A.; Harrap, K. R. *Cancer Res.* **1994**, *54*, 5618–5622.
- (35) Ghezzi, A. R.; Aceto, M.; Casino, C.; Gabano, E.; Osella, D. J. *Inorg. Biochem.* **2004**, *98*, 73–78.
- (36) Janovska, E.; Novakova, O.; Natile, G.; Brabec, V. J. *Inorg. Biochem.* **2002**, *90*, 155–158.
- (37) Ushay, H.M.; Tullius, T. D.; Lippard, S. J. *Biochemistry* **1981**, *20*, 3744–3748.
- (38) Beckford, F.; Dourth, D.; Shaloski, M., Jr; Didion, J.; Thessing, J.; Woods, J.; Crowell, V.; Gerasimchuck, N.; Gonzalez-Sarrias, A.; Seeram, N. P. *J. Inorg. Biochem.* **2011**, *105*, 1019–1029.
- (39) Beckford, F.; Thessing, J.; Woods, J.; Didion, J.; Gerasimchuck, N.; Gonzalez-Sarrias, A.; Seeram, N. P. *Metallomics* **2011**, *3*, 491–502.
- (40) Peberdy, J. P.; Malina, J.; Khalid, S.; M.J. Haman, M. J.; Rodger, A. J. *Inorg. Biochem.* **2007**, *101*, 1937–1945.
- (41) Pjura, P. E.; Grzeskowiak, K.; Dickerson, R. E. *J. Mol. Biol.* **1987**, *197*, 257–271.
- (42) Guan, Y.; Shi, R.; Li, X.; Zhao, M.; Li, Y. J. *Phys. Chem. B* **2007**, *111*, 7336–7344.
- (43) Weisblum, B.; Haenssler, E. *Chromosoma* **1974**, *46*, 255–271.
- (44) Fernandez, P.; Farre, X.; Nadal, A.; Fernández, E.; Peiro, N.; Sloane, B. F.; Sih, G.; Chapman, H. A.; Campo, E.; Cardesa, A. *Int. J. Cancer* **2001**, *95*, 51–55.
- (45) Podgorski, I.; Sloane, B. F. *Biochem. Soc. Symp.* **2003**, *70*, 263–276.
- (46) Casini, A.; Gabbiani, C.; Sorrentino, F.; Rigobello, M. P.; Geldbach, A. B. T. J.; Marrone, A.; Re, N.; Hartinger, C. G.; Dyson, P. J.; Messori, L. *J. Med. Chem.* **2008**, *51*, 6773–6781.
- (47) Spencer, J.; Casini, A.; Zava, R.; Rathnam, R. P.; Velhanda, S. K.; Pfeffer, M.; Callear, S. K.; Hursthouse, M. B.; Dyson, P. J. *Dalton Trans.* **2009**, 10731–10735.
- (48) Samari, F.; Hemmateenejad, B.; Shamsipur, M.; Rashidi, M.; Samouei, H. *Inorg. Chem.* **2012**, *51*, 3454–3464.
- (49) Chen, G. Z.; Huang, X. Z.; Xu, J. G.; Wang, Z. B.; Zhang, Z. Z. *Method of Fluorescent Analysis*, 2nd ed.; Science Press: Beijing, China, 1990; Chapter 4, p 123.
- (50) Kalaivani, P.; Prabhakaran, R.; Ramachandran, E.; Dallemer, F.; Paramaguru, G.; Renganathan, R.; Poornima, P.; Vijaya Padma, V.; Natarajan, K. *Dalton Trans.* **2012**, *41*, 2486–2499.
- (51) Mallick, A.; Chandra, S.; Maiti, S.; Chattopadhyay, N. *Biophys. Chem.* **2004**, *112*, 9–14.
- (52) Wang, Y.; Wang, X.; Wang, J.; Zhao, Y.; He, W.; Guo, Z. *Inorg. Chem.* **2011**, *50*, 12661–12666.
- (53) Yi, C.; Yang, C. J.; Liu, J.; Xu, M.; Wang, J. H.; Cao, Q. Y.; Gao, X. C. *Inorg. Chim. Acta* **2007**, *360*, 3493–3498.
- (54) Li, Z.; Xiang, Y.; Tong, A. *Anal. Chim. Acta* **2008**, *619*, 75–80.
- (55) Basu, A.; Das, G. *Dalton Trans.* **2011**, *40*, 2837–43.
- (56) Sheldrick, G. M. *SHELX-97, An integrated system for solving and refining crystal structures from diffraction data*; University of Göttingen: Göttingen, Germany, 1997.
- (57) Sluis, P.; van der Spek, A. L. *Acta Crystallogr.* **1990**, *A46*, 194–201.
- (58) Spek, A. L. *PLATON*; University of Utrecht: Utrecht, The Netherlands, 2001.
- (59) Barton, J. K.; Goldberg, J. M.; Kumar, C. V.; Turro, N. J. *J. Am. Chem. Soc.* **1986**, *108*, 2081–2088.